



ORIGINAL ARTICLE

A Au nanoparticle and polydopamine co-modified biosensor: A strategy for *in situ* and label-free surface plasmon resonance immunoassays



Bin Du^a, Xihui Mu^a, Jianjie Xu^a, Shuai Liu^a, Zhiwei Liu^a, Zhaoyang Tong^{a,*},
Zhaofeng Wu^b, Zhi-Mei Qi^c

^a State Key Laboratory of NBC Protection for Civilian, Beijing 102205, China

^b School of Physics Science and Technology, Xinjiang University, Urumqi, Xinjiang 830046, China

^c State key Laboratory of Transducer Technology, Aerospace Information Research Institute, Chinese Academy of Sciences, Beijing 100190, China

Received 9 May 2022; accepted 26 July 2022

Available online 30 July 2022

KEYWORDS

Au nanoparticles;
Biosensor;
Human IgG;
Polydopamine;
Surface plasmon resonance

Abstract This article reports a surface plasmon resonance (SPR) strategy capable of label-free yet amplified *in situ* immunoassays for sensitive and specific detection of human IgG (hIgG), a serum marker that is important for the diagnosis of certain diseases. Primarily, a wavelength-modulated Kretschman configuration SPR analyzer was constructed, and Au film SPR biosensor chips were fabricated. Specifically, based on Au nanoparticles (AuNPs) adsorbed on the surface of the Au film, the AuNP/Au film was coated with polydopamine (PDA) to fix streptavidin (SA), and then the biotinylated antibodies were connected to the surface of the biosensor chip. The SPR analyzer was utilized for *in situ* real-time monitoring of hIgG. Due to the immunological recognition between the receptor and target, the surface plasmon waves produced by the attenuated total reflection were affected by the changes in the surface of the biosensor chip. The resonance wavelength (λ_R) of the output spectra gradually redshifted, and the redshift degrees were directly related to the target concentration. The biosensor can realize the *in situ* detection of hIgG, displaying satisfactory sensitivity, excellent specificity and stability. Briefly, by monitoring the shift in λ_R after specific binding, a new SPR immunoassay can be customized for label-free, *in situ* and amplified hIgG detection. The

* Corresponding author.

E-mail address: billzytong@126.com (Z. Tong).

Peer review under responsibility of King Saud University.



operating principle of this research could be extended as a common protocol for many other targets of interest.

© 2022 The Author(s). Published by Elsevier B.V. on behalf of King Saud University. This is an open access article under the CC BY-NC-ND license (<http://creativecommons.org/licenses/by-nc-nd/4.0/>).

1. Introduction

Surface plasmon resonance (SPR) technology is a molecular biological detection technology that utilizes surface plasmon waves (SPWs) to detect changes occurring at the surface of a thin metal film (such as gold and silver films) (Nakano et al., 2001; Lakhtakia, 2007; Manera et al., 2013). The intense interaction between an incident electromagnetic (EM) wave and free-electron ensemble of the metal lead to the collective electron density oscillations which confined at the metal-dielectric interface, and SPR occurs when the energy and momentum of this incident electromagnetic wave becomes equal to that of the oscillating surface electrons in the metal (Khanikar et al., 2021). To excite SPR, several coupling structures have been applied, such as optical fibers (Li et al., 2020; Wang et al., 2017), gratings (Reiner et al., 2018; Toma et al., 2018) and prism. Compared with other coupling structures, the Kretschman configuration is the most commonly used prism-coupling (Verma and Prakash, 2015; Zhang et al., 2013; Conoci et al., 2002) excitation structure for SPR sensing devices and possesses a simple and sensitive advantage. The SPR technique is advantageous in terms of a simple, label-free, *in situ* method with economical and simple fabrication, and this technique is widely applied in current biosensors to study ligand interactions and analyses, such as binding kinetics and affinity and specificity of bioactive compounds to target structures (Sun et al., 2006; Liu et al., 2004; Zhang et al., 2015).

Although notable achievements have been obtained, the fabrication of novel SPR immunosensors using new methods to achieve sensitive, fast and facile detection is still a challenge. In particular, the construction of the sensing interface is an important factor that affects the performance of SPR immunosensors.

Because of the strong localized surface plasmon resonance (LSPR), the Au nanoparticles (AuNPs) are widely used in analysis and detection, especially in SPR analysis (Ko et al., 2009; Zhuang et al., 2015; Cai et al., 2018), due to their excellent optical properties, good surface modification, strong stability and good biocompatibility (Inci et al., 2013). Numerous materials have been used to fabricate highly sensitive sensing interfaces. An adhesive polydopamine (PDA) coating (Lee et al., 2007) is formed by dopamine self-polymerization. PDA can be easily deposited on almost all substrates and provides active sites for amine and thiol groups (Lee et al., 2009); and PDA also possesses high hydrophilicity and biocompatibility as well as compatibility with aqueous solutions, the possibility to obtain an ultrathin compact polymer film by the controlled self-limiting growth (Tretjakov et al., 2013). Thus, PDA is very suitable for use as a recognition molecular immobilization interface material for biosensors (Palladino et al., 2019; Shi et al., 2016; Lin et al., 2017; Lin et al., 2017; Ren et al., 2018).

Human immunoglobulin G (hIgG) is the main component of serum antibodies and plays a protective role in the body's immunity, which acts as an important biomarker. Although hIgG cannot represent all biomolecules, especially its concentration in serum reaches mg/mL level, low-concentration hIgG detection is of great significance, particular to provide a technical basis for the development of a biosensor that can detect low-concentration biomolecules, which has important supporting significance for the detection of various germs including the new coronavirus. Therefore, IgG was selected as the target for the development of novel biosensors in this paper.

Compared with traditional methods for IgG detection, such as enzyme-linked immunosorbent assays (Nakano and Nagata, 2003); chemiluminescence (Hacker et al., 1995), and electrophoresis (Tissot et al., 1993), SPR is relatively suitable for hIgG detection due to its

high throughput, convenient operation and wide applicability. Here, we present a novel SPR immunoassay for the *in situ* and label-free detection of hIgG. In this study, a wavelength-modulated Kretschman configuration SPR analyzer was constructed. The Au film SPR chip was modified with AuNPs and PDA. Afterward, the amplified antibody loading capacity of the biotin-avidin system (Zavaleta et al., 2007; Tsai and Wang, 2005; Leonardo et al., 2018) was utilized to fabricate the SPR biosensor chip. The AuNPs, refractive index (*n*) sensitivity of the Au film SPR chip, the morphology of the SPR biosensor chip, and the fabrication process of SPR biosensor chip were characterized. The sensitivity, specificity, regeneration and stability of this biosensor were further investigated, and the results show that the SPR biosensor developed in this article could *in situ* detect as low as 50 ng/mL hIgG with satisfactory sensitivity, excellent specificity and stability. The SPR immunoassay in this article showed that the use of AuNPs, PDA and the biotin-avidin system fully improved the sensitivity of the sensor and was an effective means to enhance the *in situ* and label-free detection performance of the biosensor. The AuNPs and self-polymerization of dopamine were used to provide a simple and quick surface modification method for the SPR biosensor, and its operating principle could be extended as a common protocol for many other targets.

2. Materials and methods

2.1. Reagents and instruments

Biotinylated goat anti-human IgG and hIgG were received from Beijing Biosynthesis Biotechnology Co., Ltd. (China). Bovine serum albumin (BSA) was purchased from Beijing Solarbio Science & Technology Co., Ltd. (China). Ovalbumin (OVA) was purchased from Shanghai Macklin Biochemical Co., Ltd. (China). Dopamine hydrochloride used for PDA polymerization was purchased from Thermo Fisher Scientific (United States). Streptavidin (SA) and poly(allylamine hydrochloride) (PAH) were received from Sigma-Aldrich Co. (USA). Diiodomethane (CH_2I_2 , $n = 1.74$) was received from J&K Scientific Ltd. (China). Phosphate buffered saline (PBS, 10 mmol/L, pH = 7.2) and Tris-HCl buffer solution (10 mmol/L, pH = 8.5) were prepared with deionized water. OVA, BSA, goat anti-human IgG, and hIgG were dissolved in PBS (10 mmol/L, pH = 7.2). All the other reagents were of analytical grade and purchased from Beijing Chemical Works (China). A 0.5 mm thick quartz wafer was used as the substrate.

A 2WJ Abbé refractometer (Shanghai CSOIF Co., Ltd., China) was used to measure the refractive indices of NaCl aqueous solutions with different mass concentrations. The particle size distribution, TEM image and absorption spectra of the AuNPs solution before and after deposition on the surface of Au/PAH film were obtained on a Zetasizer Nano-ZS nano particle analyzer (Malvern Panalytical Ltd., UK), a Tecnai G2 F30 transmission electron microscope (FEI, USA) and a BioMATE 3S UV-Vis spectrophotometer (Thermo Fisher Scientific Inc., USA), respectively. A scanning probe microscope (SPM) (SOLVER NEXT, NT-MDT Co., Russia) was used

for characterization of the surface morphologies and topographies of biosensor chips, and $1\ \mu\text{m} \times 1\ \mu\text{m}$ regions of the chips were scanned using tapping mode.

2.2. Construction of the SPR analyzer

A wavelength-modulated SPR device can provide a real-time curve of the wavelength-reflected light intensity relationship, and it can also meet the demand of miniaturization, imaging, multiple channels, multiparameter measurements, etc. (Liu et al., 2005). Fig. 1A displays the schematic diagram SPR analyzer used in this paper. The wavelength-modulated SPR analyzer works with a Kretschmann configuration to achieve the resonant condition by attenuated total reflection (ATR) (Juárez et al., 2006; Nizamov and Mirsky, 2011) in a triangular prism ($45^\circ/45^\circ/90^\circ$, Scott N-SF6 glass, $n = 1.799$ at $632.8\ \text{nm}$). The SPR chip was placed on the prism, and a sample chamber was tightly attached to the middle of the SPR chip. To increase the coupling efficiency, diiodomethane ($n = 1.74$) was introduced between the prisms and the SPR chip as an index-matching liquid. Ultimately, the sample chamber, SPR chip and prism were sandwiched, and the three were placed on a precision rotating stage to adjust the optical path. The broadband light generated by a tungsten-halogen lamp (LS-1, Ocean Optics, USA) successively passed through a multimode quartz fiber, collimator and linear polarizer and then became p -polarized parallel light. Afterward, p -polarized parallel light entered the prism at an angle ($\theta = 13^\circ$) with respect to the prism surface normal, and the evanescent field caused by ATR penetrated through the glass/metal interface to excite the surface plasmon mode at the metal/medium interface of the SPR chip at a specific wavelength, which was named the

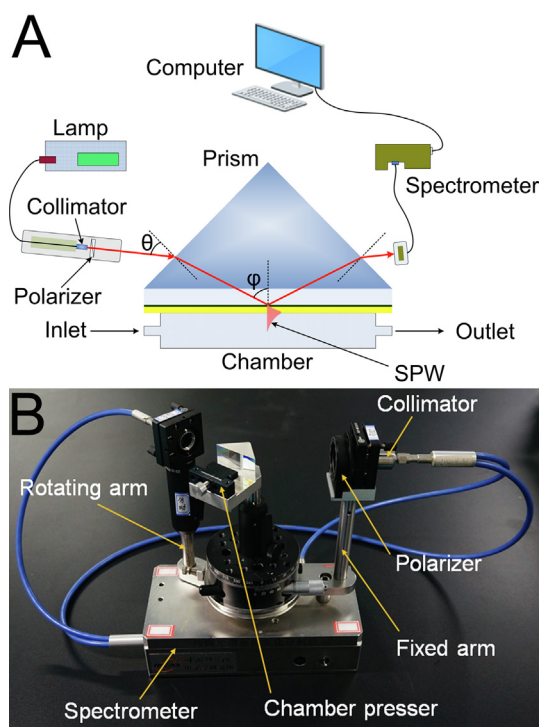


Fig. 1 Schematic diagram (A) and photograph (B) of the wavelength-modulated SPR analyzer.

resonance wavelength (λ_R). The total reflection beam output from another side of the prism was transmitted to a spectrometer (USB 2000+, Ocean Optics, USA) through another collimator and another quartz fiber, and the spectra were recorded for the measurement. A photograph of the SPR analyzer is shown in Fig. 1B.

2.3. Fabrication of the SPR biosensor chip

Compared with the traditional Frens trisodium citrate reduction method (Frens, 1973), the microwave method for the synthesis of AuNPs is simple and efficient and can heat the material uniformly, evenly disperse the nanoparticles, control the particle size, and shorten the nucleation time (Xu et al., 2019). First, 100 mL of 0.01 % chloroauric acid aqueous solution was placed in a microwave oven and heated for 3 min at a power of 700 W to boil the solution. Subsequently, 3 mL of 1 % trisodium citrate aqueous solution was quickly added to the boiling solution and heated for 3 min at a power of 400 W, and the solution changed from colorless to deep red under boiling. After heating, the volume of solution was adjusted to 100 mL with distilled water to maintain the concentration of AuNPs.

The Au film SPR chips were prepared by successive sputtering of a 5 nm chromium layer and a 45 nm gold film on a 0.5 mm thick quartz wafer with area $15\ \text{mm} \times 15\ \text{mm}$, and then the SPR chip was washed with distilled water and ethanol to clean the Au film for the next modification. The method of nanoparticle film deposition followed the steps depicted in Fig. 2 as follows: the Au film SPR chip was immersed in 2 mg/mL positively charged polymer PAH for 5 min and then washed and dried (Bubniene et al., 2014). Subsequently, the chip was immersed into a solution containing negatively charged AuNP nanoparticles for 5 min; after deposition of the AuNPs, the Au/PAH/AuNP film SPR chip was washed and dried. In the process of biological modification, the SPR biosensor chip was then modified with a biological crosslinked PDA membrane by the surface functionalization method. The Au/PAH/AuNP film SPR chip obtained was immersed in a

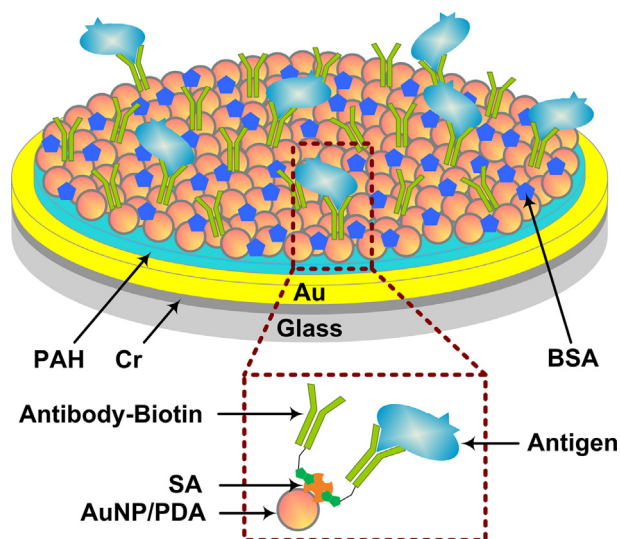


Fig. 2 Schematic diagram of the SPR biosensor chip structure.

solution of dopamine (2 mg/mL of 10 mmol/L Tris buffer, pH = 8.5) for 10 min at room temperature, and dopamine was oxidatively self-polymerized to form a certain thickness of PDA membrane and coated the surface of the SPR chip. Then, the Au/PAH/AuNP/PDA film SPR chip was rinsed with deionized water to remove the large PDA particles. Next, 50 $\mu\text{g/mL}$ SA solution was added to the surface of the Au/PAH/AuNP/PDA film of the SPR chip for 5 min, and SA was immobilized by covalent binding between the amino groups of SA and the quinone group of PDA. Then, the unbound SA was washed away with PBS. Subsequently, biotinylated goat anti-human IgG solution (0.2 mg/mL) was dropped on the surface for 0.5 h to connect the biotin group of the antibody to SA. After the reaction was completed, unbound antibodies were washed with PBS buffer, and the obtained SPR biosensor chip surface was blocked with 1 mg/mL BSA. Combining biotin-avidin technology with AuNPs' excellent optical characteristics and large specific surface area, the fixed amount of biorecognition molecules can be amplified, which improves the sensitivity of SPR to detect biomolecules.

2.4. Immunoassay and simulated samples measurements

Immunoassays were performed by analyzing a series of hIgG solutions with different concentrations using the SPR biosensor chip immobilized with goat anti-human IgG. The sensitivity of the sensor was evaluated by monitoring the $\Delta\lambda_R$ caused by the binding reaction of the antigen and antibody. First, the obtained SPR biosensor chip was fixed on the SPR analyzer, and the sample chamber was pressed on the chip tightly. The PBS solution was injected to stabilize the baseline, hIgG solution was added to the chamber for immunoassay, and real-time changes in SPR spectra were monitored. After 30 min, the sample solution was washed with PBS solution three times to remove unbound antigen and maintained a steady λ_R ; ultimately, the λ_R shifts caused by the interactions between the antibody and antigen were determined. All experiments were performed at room temperature and conducted in triplicate to examine the reliability of the assays. To evaluate the biosensor specificity of hIgG, BSA and OVA were determined by the same procedure as was utilized to detect hIgG. After the SPR biosensor was washed with PBS buffer, BSA (1 mg/mL), OVA (1 mg/mL) and hIgG (5 $\mu\text{g/mL}$) were added to the sample chamber and incubated for 30 min. After the specificity test, the SPR biosensor was washed three times with PBS buffer to wash away the nonspecifically bound analytes, and the changes in the SPR spectra before and after the sample addition were recorded.

Although hIgG exists in blood, it should be noted that the SPR biosensor developed in this paper can be extended to the detection of other biomolecules such as various pathogens in the future. Therefore, it is necessary to evaluate the actual detection performance of the SPR biosensor for various possible complex simulated samples. Soil (1 g), lake water (1 mL) and rabbit serum (80 μL) were added to 160 μL of 100 $\mu\text{g/mL}$ hIgG standards. Then, the mixture was diluted to 8 mL with PBS to obtain a final hIgG concentration of 2 $\mu\text{g/mL}$. Rabbit blood samples of 1 mL were collected from normal rabbits. The rabbit blood was then centrifuged at 1,000 g for 5 min at 4 $^{\circ}\text{C}$. The upper layer of serum was collected in clean

tubes and stored at -20°C before further experiment. The lake water and rabbit serum samples were measured directly. The soil sample was centrifuged at 5000 g for 15 min, the supernatants were collected, and the recovery rate, relative standard deviation (RSD) and other indices of detection were analyzed and calculated.

2.5. Stability and regeneration

The PBS solution was injected into the sample chamber, and the changes in the SPR spectra with time were observed. The spectra were recorded every 10 min for a total of 2 h. When the immunoassay was finished, the biosensor chip was thoroughly cleaned separately with piranha solution ($\text{H}_2\text{SO}_4:30\% \text{H}_2\text{O}_2 = 7:3 \text{ V/V}$) and distilled water and then dried. The results show that the Au film could be utilized repeatedly.

3. Results

3.1. Topography and refractive index sensitivity of the Au film SPR chip

The surface morphology and topography of the as-prepared SPR biosensor chip were determined using a SOLVER NEXT scanning probe microscope. For comparison, AFM images of the Au film, Au/PAH/AuNP film and Au/PAH/AuNP/PDA film are also given in Fig. 3. Fig. 3A clearly shows that the surface of the Au film without any modification is very smooth, and its root-mean-square (RMS) roughness is 0.21 nm. When AuNPs were absorbed on the Au film through positive and negative charge interactions, particles were irregularly and densely distributed on the chip surface (Fig. 3B). Particles and interface analysis show that these particles have a size of ~ 18 nm. Combined with the particle size analysis of AuNPs above, it shows that AuNPs are well distributed on the chip surface. As seen from Fig. 3C, after AuNPs and exposed areas on the chip surface coated with PDA, the number of particles on the chip surface decreased, and the morphology became smooth, indicating that dopamine polymerized *in situ* at each location on the chip surface, making the Au film modified by AuNP/PDA smooth compared to the Au film modified by AuNPs. When goat anti-human IgG was fixed by the biotin-avidin system, the surface of the chip became rougher, and the fixed antibodies were distributed between AuNPs (Fig. 3D). AFM characterization shows that this method successfully fixes goat anti-human IgG to the surface of the biosensor chip through the biotin-avidin system.

The refractive indices of NaCl aqueous solution with a weight concentration in the range of 1 wt% to 15 wt% were measured, and the corresponding refractive indices ranged from 1.335 to 1.356 (Supplementary Fig. S1). As shown in Fig. 4, when the refractive indices of the NaCl aqueous solutions to be measured in the sample cell gradually increased, the λ_R of the resonance spectra redshifted accordingly. After plotting the value of resonance wavelength shift ($\Delta\lambda_R$) and the refractive indices of the NaCl aqueous solutions (n) to be plotted (Supplementary Fig. S2), the following linear relationship was obtained:

$$\Delta\lambda_R = 4295n - 5727.4 \quad (R^2 = 0.997, N = 7).$$

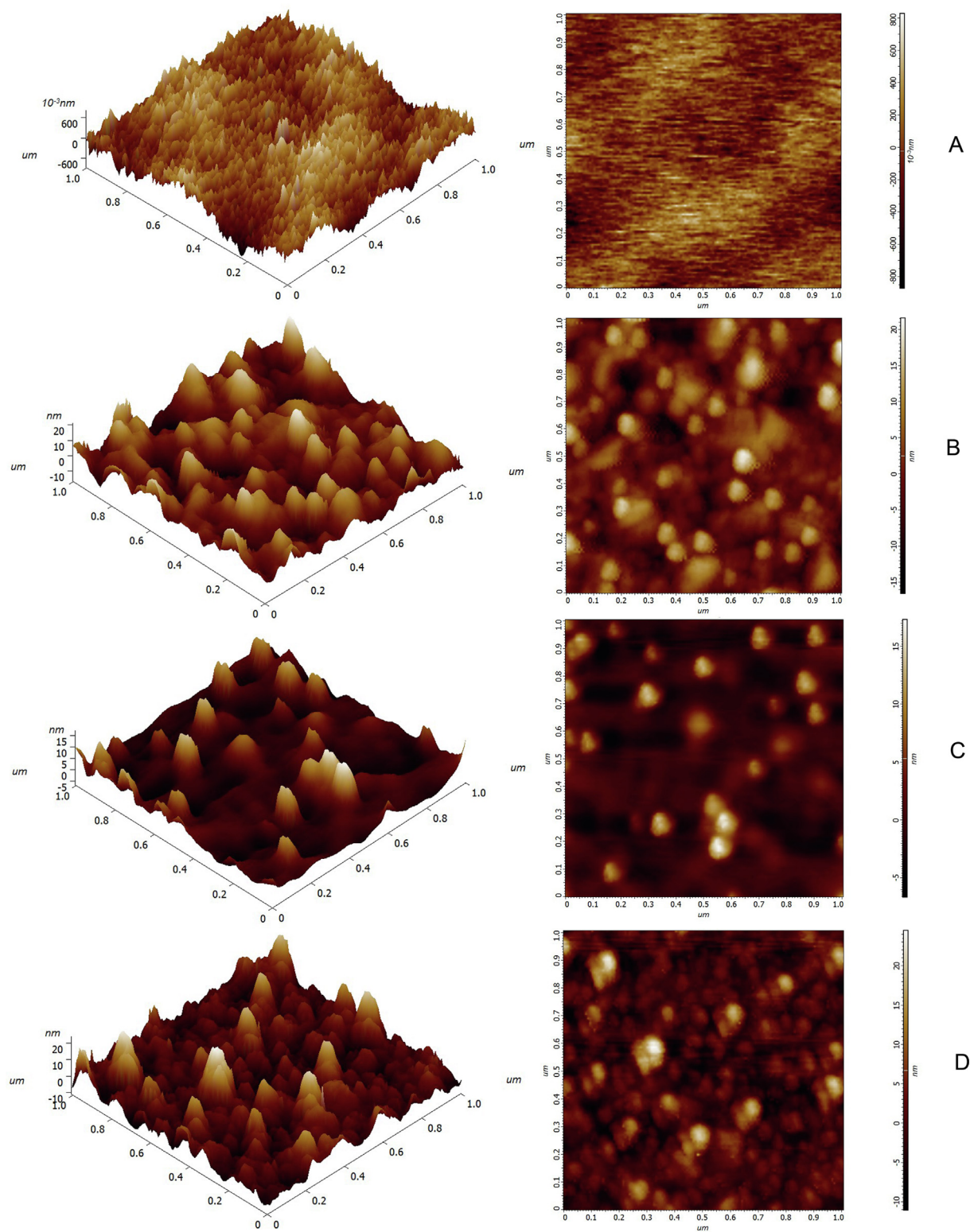


Fig. 3 AFM image ($1 \mu\text{m} \times 1 \mu\text{m}$) of the surfaces of Au film (A), Au/PAH/AuNP film (B), Au/PAH/AuNP/PDA film (C), and SPR.

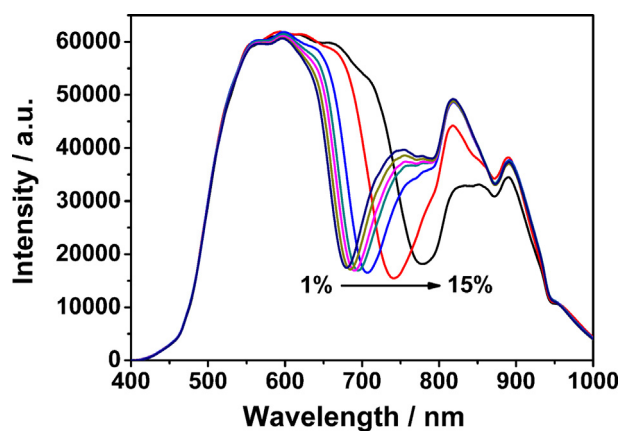


Fig. 4 The resonance spectra of the Au film SPR sensor in NaCl solutions with varying concentrations.

The refractive index sensitivity of the Au film SPR chip was $4295 \text{ nm}\cdot\text{RIU}^{-1}$, which indicated that the Au film SPR chip has high sensitivity (Zhang et al., 2012; Wang et al., 2021).

3.2. AuNPs and SPR biosensor chip

According to the particle size distribution and TEM image, the particle size of AuNPs prepared by the microwave method in this experiment was $\sim 18 \text{ nm}$ (Supplementary Fig. S3 and Fig. S4). The UV-Vis absorption spectra show that about $366 \mu\text{g}$ of AuNPs were adsorbed on the surface, meanwhile the characteristic absorption peak is located at 520 nm (Supplementary Fig. S5), which is largely consistent with the literature reports (Ye et al., 2012; Joshi et al., 2013) and indicates that AuNPs prepared by the microwave method have a uniform particle size. The resonance spectra changes of the SPR biosensor chip during the modification process were measured, and the resonance spectra of the Au film SPR chip, Au/PAH/AuNP film, and Au/PAH/AuNP/PDA film on water were measured on the SPR analyzer. Fig. 5 displays SPR spectra measured at $\theta = -13^\circ$ with the Au film, Au/PAH/AuNP film

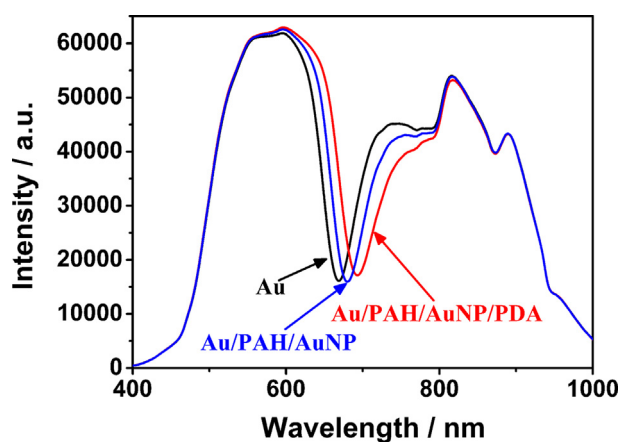


Fig. 5 Changes in the resonance spectra of water on the SPR chip before and after modification with AuNPs/PAH and PDA at an angle of incidence $\theta = 13^\circ$.

and Au/PAH/AuNP/PDA in water, from which the λ_R of the Au film was determined to be 668.71 nm and redshifted to 680.41 nm after AuNPs were absorbed to the Au film by positive and negative charge interactions with PAH, and the $\Delta\lambda_R$ was 11.7 nm . Such a large shift in λ_R indicated that AuNPs were successfully deposited on the Au film. After the chip was coated with PDA for 10 min, its redshifted $\Delta\lambda_R$ was 13.14 nm .

Subsequently, SA was coupled to the chip surface by the reaction of the amino group and PDA. SA with different concentrations were added to the surface of Au/PAH/AuNP/PDA film, and the optimal concentration of SA was $50 \mu\text{g}/\text{mL}$ (Table S1). When biotinylated goat anti-human IgG was conjugated on the surface of the SA-immobilized chip, the λ_R resulting from the immobilization of the antibodies onto the chip surface due to avidin-biotin interaction was monitored. Fig. 6A shows the real-time change in resonance spectra of goat anti-human IgG coupled on the surface of Au/PAH/AuNP/PDA/SA film within 60 min. The extended λ_R gradually redshifted, indicating that the biotinylated goat anti-human IgG was loaded onto the chip surface by the biotin-avidin reaction. A real-time change graph of $\Delta\lambda_R$ was plotted and is shown in Fig. 6B. At the initial stage of immobilization, λ_R redshifted rapidly, indicating that the antibody was rapidly coupled to the surface of the Au/PAH/AuNP/PDA/SA film. As the coupling progressed, the λ_R redshift rate decreased significantly after 30 min, which indicated that the SA immobilized on the PDA surface had gradually bound and saturated with the antibody, and the antibody binding rate decreased gradually and finally reached an equilibrium state. The linear

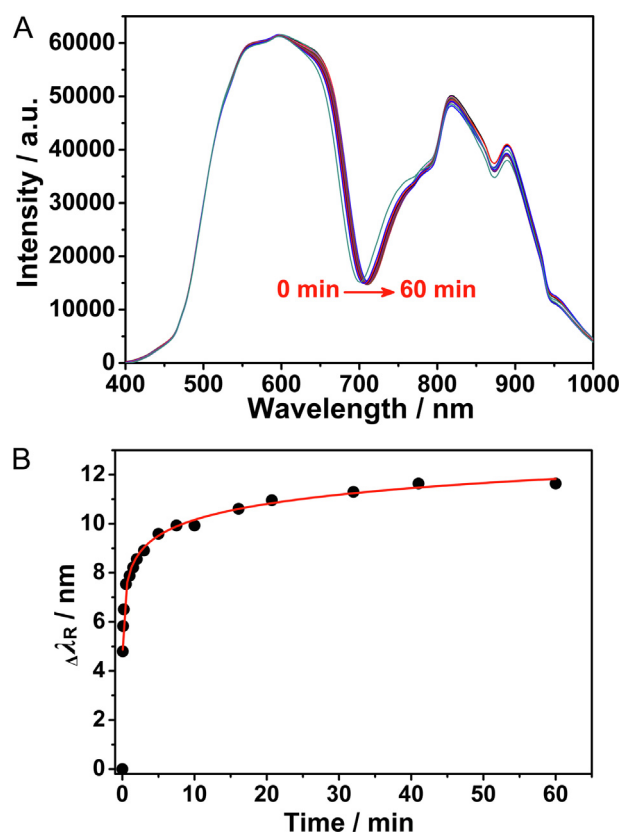


Fig. 6 Real-time change of SPR spectra when antibody immobilized on the sensor chip (A) and kinetic curve of goat anti.

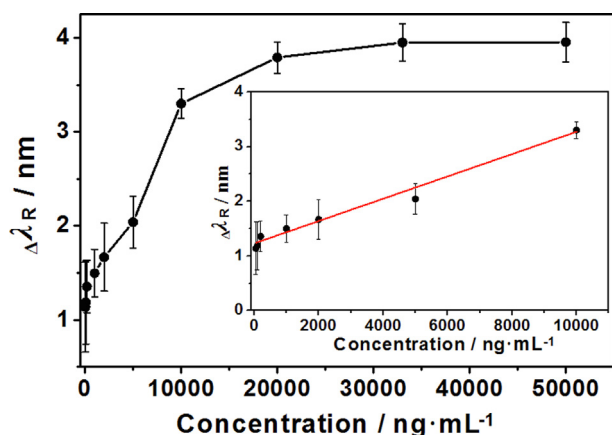


Fig. 7 Resonance wavelength shifts of the SPR biosensor by detecting different concentrations of hIgG and calibration curve for hIgG detection by the SPR biosensor.

relationship of $\Delta\lambda_R$ with biotinylated goat anti-human IgG coupling time T was as follows:

$$\Delta\lambda_R = 0.963\ln T + 7.938 \quad (R^2 = 0.995, P < 0.0001, N = 17).$$

The change in UV-Vis absorption spectra of biotinylated goat anti-human IgG solution before and after coupling on the surface of the Au/PAH/AuNPs/PDA/SA film was also determined. After antibody immobilization, the absorption peak at 280 nm decreased significantly (Supplementary Fig. S6), which indicated that the 3.2 μg of antibody bound to SA and immobilized on the surface of the SPR biosensor chip; thus, the concentration of residual antibody solution decreased.

3.3. Determination of hIgG

In this paper, the SPR biosensor response to hIgG solutions with different concentrations was recorded. Fig. S7 displays the change in the SPR spectra before and after the detection of a 1 $\mu\text{g}/\text{mL}$ hIgG solution. The λ_R of the blank sample (PBS solution) was 717.94 nm; when the sample was replaced with a 1 $\mu\text{g}/\text{mL}$ hIgG solution, λ_R gradually redshifted, and after 30 min, $\Delta\lambda_R$ was 1.2 nm. As shown in Fig. 7, the SPR biosensor shows a good response to hIgG in the concentration range of 50 ng/mL \sim 50 $\mu\text{g}/\text{mL}$. It could be noted that the biosensor still responded with a concentration of hIgG as low as 50 ng/mL, and its detection limit (LOD) was 50 ng/mL. Moreover, when the hIgG concentration reached 20 $\mu\text{g}/\text{mL}$, the response intensity of the biosensor reached the maximum value. The SPR biosensor showed a linear response to hIgG in the concentration range of 50 ng/mL \sim 10 $\mu\text{g}/\text{mL}$. The curve of the concentration of the hIgG solution (C_{hIgG})

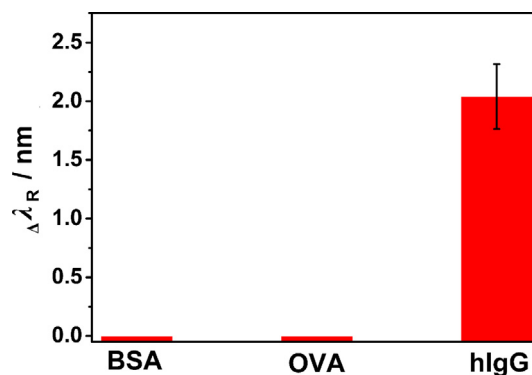


Fig. 8 Response of SPR biosensor to different proteins.

and $\Delta\lambda_R$ is presented in Fig. 7 (insert graph), and the following relation was obtained:

$$\Delta\lambda_R = 2.041 \times 10^{-4} C_{\text{hIgG}} + 1.229 \quad (R^2 = 0.987, P < 0.00001, N = 7).$$

The practical value and analytical performance of the developed SPR biosensor were evaluated by simulating samples at the same hIgG concentration. The soil, lake water and rabbit serum samples containing 2 $\mu\text{g}/\text{mL}$ hIgG were injected into the chamber, and the $\Delta\lambda_R$ was recorded. The measured values were obtained by the regression equation (Table 1). The designed biosensor met the requirements for analysis of the simulated samples above; its RSDs below 10 % and recovery rates (between 94.45 % and 108.45 %) were acceptable, indicating that the designed SPR biosensor is feasible for detecting complex biological samples.

3.4. Specificity, stability and regeneration of hIgG detection

Specificity capabilities were investigated by measuring the response of the SPR biosensor to different proteins. Fig. 8 shows the $\Delta\lambda_R$ before and after the sensor detected BSA, OVA and hIgG. The $\Delta\lambda_R$ of 5 $\mu\text{g}/\text{mL}$ hIgG was 1.72 nm, while BSA and OVA had almost no influence on the detection of hIgG. This phenomenon is due to antigen-antibody specific binding between goat anti-human IgG and hIgG, indicating that the SPR biosensor can specifically detect target molecules.

Stability is one of the critical evaluation indicators of biosensors. The stability of the sensor's output signal is related to the accuracy of the detection results. This article evaluated the stability of SPR biosensors over a period of time. Fig. S8 shows the superposition of all resonance spectra within 2 h. These results suggest that the λ_R of the PBS solution was virtually unchanged within 2 h, remaining at 712.1 nm. The output light intensity only fluctuated slightly at this wavelength. This result indicates that the biotin-avidin-immobilized goat anti-human IgG on the sensitive film of the sensor did not

Table 1 Analytical results of hIgG in simulated samples (N = 4).

Sample	Added ($\mu\text{g}/\text{mL}$)	Found ($\mu\text{g}/\text{mL}$)	Recovery (%)	RSD (%)
soil	2	1.889	94.45	6.83
fresh water	2	1.938	96.88	7.51
rabbit serum	2	2.169	108.45	4.92

Table 2 Comparison of different SPR sensors for IgG *in-suit* detection.

Target	Modified material	Recognition molecule	Range/LOD	Ref.
hIgG	SiO ₂ sol-gel film/AuNPs	rabbit anti-human IgG	0.30 ~ 40.00 µg/mL	(Jian et al., 2010)
mouse IgG	MoS ₂ nanoflower/AuNPs	goat anti-mouse IgG	5 ~ 200 µg/mL	(Zhao et al., 2020)
goat anti-human IgG	AuNP/GBP-ProA	hIgG	0.06 µg/mL	(Ko et al., 2009)
hIgG	PoPD/AuNPs	goat anti-human IgG	1.0 ~ 150 µg/ml	(Wang et al., 2008)
			0.8 ~ 38.5 µg/mL	
			0.1 µg/mL	
hIgG	PDA	goat anti-human IgG	2 ~ 250 µg/mL	(Du et al., 2020)
				Previous work
hIgG	PAH/AuNP/PDA/SA	goat anti-human IgG	50 ng/mL ~ 10 µg/mL	This work
			50 ng/mL	

detach. That is, the sensitive film remained stable and could be utilized stably for a certain period of time.

The SPR biosensor chip was immersed in piranha solution to clean the Au film and then rinsed repeatedly with ethanol and distilled water. The SPR spectra of the cleaned SPR biosensor chip and the unused Au film SPR chip against water were measured at the same incident angle (Supplementary Fig. S9), and the results clearly showed that after regeneration, the λ_R of the tested chip was basically returned to the position of the unused Au film SPR chip. Then the regenerated Au film SPR chip can be modified to fabricate SPR biosensor chip, and the cycle can be repeated at least 5 times. This result indicates that the prepared SPR biosensor chip can be reused, lowering detection costs.

In brief, AuNPs and PDA were used as the interface modification materials of the sensor, the biotin-avidin system was used to increase the antibody loading, and a new method for functionalization of the SPR biosensor chip was developed. Compared with our previous work, the LOD of the SPR biosensor developed in this article is approximately 40-fold lower than that of the sensor modified with PDA film and then conjugated with antibody, and compared with other SPR sensors for hIgG *in situ* detection, the SPR biosensor exhibits comparable simplification and convenience, as well as satisfactory sensitivity (Table 2).

4. Conclusion

In summary, a novel SPR immunoassay was proposed. A Kretschmann prism-type SPR *in situ* biochemical analyzer based on ATR was set up, and then AuNPs were absorbed on the Au film SPR chip through charge interaction. Afterward, the surface of the chip was coated with PDA. Finally, SA was immobilized on the surface of the PDA membrane, and a biotin-avidin system was utilized to connect biotin-labeled goat anti-human IgG. The modification processes and surface morphology of the SPR biosensor chip were characterized by resonance spectra and AFM, respectively. During the detection process of hIgG, the immune reaction caused a change in the refractive index of the sensitive membrane, which in turn caused λ_R to shift. The immunoassay of hIgG shows that the biosensor can realize the *in situ* detection of hIgG at concentrations as low as 50 ng/mL, and the $\Delta\lambda_R$ of the SPR spectra is directly related to the target concentration in the range of 50 ng/mL ~ 10 µg/mL. This research provides a simple and effective approach for the establishment of a sensitive SPR immunoassay, and this study also provides a scientific basis for the future development of highly sensitive and specific optical biosen-

sors suitable for biomolecular detection, which has important supporting significance for the detection of various germs including the new coronavirus.

Declaration of Competing Interest

The authors declare that they have no known competing financial interests or personal relationships that could have appeared to influence the work reported in this paper.

Acknowledgments

This research was funded by the Foundation of State Key Laboratory of NBC Protection for Civilian (SKLNBC2020-03, SKLNBC2020-07, SKLNBC2019-05).

Appendix A. Supplementary material

Supplementary data to this article can be found online at <https://doi.org/10.1016/j.arabjc.2022.104158>.

References

- Bubniene, U., Oćwieja, M., Bugelyte, B., Adamczyk, Z., Nattich-Rak, M., Voronovic, J., Ramanaviciene, A., Ramanavicius, A., 2014. Deposition of gold nanoparticles on mica modified by poly (allylamine hydrochloride) monolayers. *Colloids Surf. A* 441, 204–210.
- Cai, G., Yu, Z., Ren, R., Tang, D., 2018. Exciton-plasmon interaction between AuNPs/graphene nanohybrids and CdS quantum dots/TiO₂ for photoelectrochemical aptasensing of prostate-specific antigen. *ACS Sens.* 3, 632–639.
- Conoci, S., Palumbo, M., Pignataro, B., Rella, R., Valli, L., Vasapollo, G., 2002. Optical recognition of organic vapours through ultrathin calix[4]pyrrole films. *Colloids Surf. A* 198–200, 869–873.
- Du, B., Tong, Z., Mu, X., Xu, J., Liu, S., Liu, Z., Qi, Z., 2020. A polydopamine-modified wavelength modulated SPR biosensor for human IgG *in-situ* detection. *Basic Clin. Pharmacol. Toxicol.* 127 (S7), 75.
- Frens, G., 1973. Controlled nucleation for theregulation of the particle size in monodisperse gold suspensions. *Nat. Phys. Sci.* 241, 20–22.
- Hacker, A., Hinterleitner, M., Shellum, C., Gübitz, G., 1995. Development of an automated flow injection chemiluminescence immunoassay for human immunoglobulin G. *Fresenius J. Anal. Chem.* 352, 793–796.
- Inci, F., Tokel, O., Wang, S.Q., Gurkan, U.A., Tasoglu, S., Kuritzkes, D.R., Demirci, U., 2013. Nanoplasmonic quantitative detection of

- intact viruses from unprocessed whole blood. *ACS Nano* 7, 4733–4745.
- Jian, W., Wang, L., Sun, Y., Zhu, X., Cao, Y., Wang, X., Zhang, H., Song, D., 2010. Surface plasmon resonance biosensor based on Au nanoparticle in titania sol-gel membrane. *Colloids Surf. B* 75, 520.
- Joshi, V.G., Chindera, K., Singh, A.K., Sahoo, A.P., Dighe, V.D., Thakuria, D., Tiwari, A.K., Kumar, S., 2013. Rapid label-free visual assay for the detection and quantification of viral RNA using peptide nucleic acid (PNA) and gold nanoparticles (AuNPs). *Anal. Chim. Acta* 795, 1–7.
- Juárez, M.R., Aguirre, N.M., Pérez, L.M., Garibay-Febles, V., Lozada-Cassou, M., Becerril, M., Angel, O.Z., 2006. Optical characterization of polyethylene and cobalt phthalocyanine ultrathin films by means of the ATR technique at surface plasmon resonance. *Phys. Status Solidi A* 203, 2506–2512.
- Khanikar, T., De, M., Singh, V.K., 2021. A review on infiltrated or liquid core fiber optic SPR sensors. *Photonic. Nanostruct.* 46, 100945.
- Ko, S., Park, T.J., Kim, H.S., Kim, J.H., Cho, Y.J., 2009. Directed self-assembly of gold binding polypeptide-protein A fusion proteins for development of gold nanoparticle-based SPR immunosensors. *Biosens. Bioelectron.* 24, 2592–12397.
- Lakhtakia, A., 2007. Surface-plasmon wave at the planar interface of a metal film and a structurally chiral medium. *Opt. Commun.* 291, 279–291.
- Lee, H., Dellatore, S.M., Miller, W.M., Messersmith, P.B., 2007. Mussel-inspired surface chemistry for multifunctional coatings. *Science* 318, 426–430.
- Lee, H., Rho, J., Messersmith, P.B., 2009. Facile Conjugation of biomolecules onto surfaces via mussel adhesive protein inspired coatings. *Adv. Mater.* 21, 431–434.
- Leonardo, S., Kilcoyne, J., Samdal, I.A., Miles, C.O., O'Sullivan, C. K., Diogène, J., Campàs, M., 2018. Detection of azaspiracids in mussels using electrochemical immunosensors for fast screening in monitoring programs. *Sens. Actuators, B* 262, 818–827.
- Li, W., Zhang, A., Cheng, Q., Sun, C., Li, Y., 2020. Theoretical analysis on SPR based optical fiber refractive index sensor with resonance wavelength covering communication C+L band. *Optik* 213, 164696.
- Lin, Z., Li, M., Lv, S., Zhang, K., Lu, M., Tang, D., 2017. In situ synthesis of fluorescent polydopamine nanoparticles coupled with enzyme-controlled dissolution of MnO₂ nanoflakes for a sensitive immunoassay of cancer biomarkers. *J. Mater. Chem. B* 5, 8506–8513.
- Lin, Y., Zhou, Q., Tang, D., 2017. Dopamine-loaded liposomes for in-situ amplified photoelectrochemical immunoassay of AFB1 to enhance photocurrent of Mn²⁺-doped Zn₃(OH)₂V₂O₇ nanobelts. *Anal. Chem.* 89, 11803–11810.
- Liu, X., Sun, Y., Song, D., Zhang, Q., Tian, Y., Bi, S., Zhang, H., 2004. Sensitivity-enhancement of wavelength-modulation surface plasmon resonance biosensor for human complement factor 4. *Anal. Biochem.* 333, 99–104.
- Liu, X., Song, D., Zhang, Q., Tian, Y., Ding, L., Zhang, H., 2005. Wavelength-modulation surface plasmon resonance sensor. *TrAC-Trends Anal. Chem.* 24, 887–893.
- Manera, M.G., Ferreira-Vila, E., Garcia-Martin, J.M., Cebollada, A., Garcia-Martin, A., Giancane, G., Valli, L., Rella, R., 2013. Enhanced magneto-optical SPR platform for amine sensing based on Zn porphyrin dimers. *Sens. Actuators, B* 182, 232–238.
- Nakano, T., Nagata, A., 2003. ELISAs for free light chains of human immunoglobulins using monoclonal antibodies: comparison of their specificity with available polyclonal antibodies. *J. Immunol. Methods* 275, 9–17.
- Nakano, T., Kobayashi, H., Kaneko, F., Shinbo, K., Kato, K., Kawakami, T., Wakamatsu, T., 2001. Detection of evanescent fields on arachidic acid LB films on Al films caused by resonantly excited surface plasmons. *Stud. Interface Sci.* 11, 43–53.
- Nizamov, S., Mirsky, V.M., 2011. Self-referencing SPR-biosensors based on penetration difference of evanescent waves. *Biosens. Bioelectron.* 28, 263–269.
- Palladino, P., Bettazzi, F., Scarano, S., 2019. Polydopamine: surface coating, molecular imprinting, and electrochemistry—successful applications and future perspectives in (bio)analysis. *Anal. Bioanal. Chem.* 411, 4327–4338.
- Reiner, A.T., Fossati, S., Dostalek, J., 2018. Biosensor platform for parallel surface plasmon-enhanced epifluorescence and surface plasmon resonance detection. *Sens. Actuators, B* 257, 595–601.
- Ren, R., Cai, G., Yu, Z., Zeng, Y., Tang, D., 2018. Metal-polydopamine framework: an innovative signal-generation tag for colorimetric immunoassay. *Anal. Chem.* 90, 11099–11105.
- Shi, S., Wang, L., Wang, A., Huang, R., Ding, L., Su, R., Qi, W., He, Z., 2016. Bioinspired fabrication of optical fiber SPR sensors for immunoassays using polydopamine-accelerated electroless plating. *J. Mater. Chem. C* 4, 7554–7562.
- Sun, Y., Liu, X., Song, D., Tian, Y., Bi, S., Zhang, H., 2006. Sensitivity enhancement of wavelength modulation surface plasmon resonance biosensor by improving the baseline solution. *Anal. Chim. Acta* 569, 21–26.
- Tissot, J.D., Schneider, P., Hohlfeld, P., Spertini, F., Hochstrasser, D. F., Duchosal, M.A., 1993. Two-dimensional electrophoresis as an aid in the analysis of the clonality of immunoglobulins. *Electrophoresis* 14, 1366–1371.
- Toma, M., Izumi, S., Tawa, K., 2018. Rapid and sensitive detection of neuron specific enolase with a polydopamine coated plasmonic chip utilizing a rear-side coupling method. *Analyst* 143, 858–864.
- Tretjakov, A., Syritski, V., Reut, J., Boroznjak, R., Volobujeva, O., Öpik, A., 2013. Surface molecularly imprinted polydopamine films for recognition of immunoglobulin G. *Microchim. Acta* 180, 1433–1442.
- Tsai, W.B., Wang, M.C., 2005. Effect of an avidin-biotin binding system on chondrocyte adhesion, growth and gene expression. *Biomaterials* 26, 3141–3151.
- Verma, A., Prakash, A., 2015. Tripathi R. Sensitivity enhancement of surface plasmon resonance biosensor using graphene and air gap. *Opt. Commun.* 357, 106–112.
- Wang, Y., Li, S., Guo, Y., Zhang, S., Li, H., 2021. Surface plasmon polariton high-sensitivity refractive index sensor based on MMF-MOF-MMF structure. *Infrared Phys. Technol.* 114, 103685.
- Wang, W., Mai, Z., Chen, Y., Wang, J., Li, L., Su, Q., Li, X., Hong, X., 2017. A label-free fiber optic SPR biosensor for specific detection of C-reactive protein. *Sci. Rep.* 7, 16904.
- Wang, Q., Tang, H., Xie, Q., Jia, X., Zhang, Y., Tan, L., Yao, S., 2008. The preparation and characterization of poly(*o*-phenylenediamine)/gold nanoparticles interface for immunoassay by surface plasmon resonance and electrochemistry. *Colloids Surf. B* 63, 254.
- Xu, Y., Du, C., Steinkruger, J.D., Zhou, C., Yang, S., 2019. Microwave-assisted synthesis of AuNPs/CdS composite nanorods for enhanced photocatalytic hydrogen evolution. *J. Mater. Sci.* 54, 6930–6942.
- Ye, C., Zhao, Y.Y., Chen, R., Jiang, X.Y., 2012. Interactions and applications of gold nanoparticles-protein. *Sci. Sin. Chim.* 42, 1672–1682.
- Zavaleta, C.L., Phillips, W.T., Soundararajan, A., Goins, B.A., 2007. Use of avidin/biotin-liposome system for enhanced peritoneal drug delivery in an ovarian cancer model. *Int. J. Pharm.* 337, 316–328.
- Zhang, Z., Liu, J., Qi, Z.M., Lu, D.F., 2015. In situ study of self-assembled nanocomposite films by spectral SPR sensor. *Mater. Sci. Eng. C* 51, 242–247.
- Zhang, H., Song, D., Gao, S., Zhang, H., Zhang, J., Sun, Y., 2013. Enhanced wavelength modulation SPR biosensor based on gold nanorods for immunoglobulin detection. *Talanta* 115, 857–862.
- Zhang, Z., Lu, D.f., Liu, Q., Qi, Z.m. Yang, L., Liu, J., 2012. Wavelength-interrogated surface plasmon resonance sensor with

- mesoporous-silica-film-enhanced sensitivity to small molecules. *Analyst* 137, 4822-4828
- Zhao, P., Chen, Y., Chen, Y., Hu, S., Chen, H., Xiao, W., Liu, G., Tang, Y., Shi, J., He, Z., 2020. A MoS₂ nanoflower and gold nanoparticle-modified surface plasmon resonance biosensor for a sensitivity-improved immunoassay. *J. Mater. Chem. C* 8, 6861.
- Zhuang, J., Lai, W., Xu, M., Qian Zhou, Q., Tang, D., 2015. Plasmonic AuNP/g-C₃N₄ nanohybrid-based photoelectrochemical sensing platform for ultrasensitive monitoring of polynucleotide kinase activity accompanying DNase-catalyzed precipitation amplification. *ACS Appl. Mater. Interfaces* 7, 8330-8338.